ELSEVIER

International Journal of Mass Spectrometry 204 (2001) 143–157

International Journal of Mass Spectrometry

Photodissociation measurements of bond dissociation energies: $D_0(Al_2\text{-}Al)$, $D_0(TiO^+\text{-}Mn)$, and $D_0(V_2^+\text{-}V)$

Zhenwen Fu, Larry M. Russon, Michael D. Morse, P.B. Armentrout

Department of Chemistry, University of Utah, Salt Lake City, Utah 84112, USA

Abstract

The bond dissociation energies $D_0(Al_2\text{–}Al) = 2.701(5)$, $D_0(TiO^+\text{–}Mn) = 1.7629(12)$, and $D_0(V_2^+\text{–}V) = 2.323(1)$ eV have been measured from the sudden onset of predissociation in the photodissociation spectra of Al_3, $TiOMn^+$, and V_3^+. For Al_3, the predissociation threshold was observed in a spectrum arising from the metastable $^4A_2$ state (in C_{2v} symmetry), and the value of $D_0(Al_2\text{–}Al) = 2.701(5)$ eV was obtained by adding the energy of the $^4A_2$ state to the measured predissociation threshold. For $TiOMn^+$, there is currently no evidence that the predissociation threshold arises from a metastable excited electronic state; nor is there evidence that dissociation at the ground separated fragment limit fails to occur. Therefore, the predissociation threshold is taken to be the bond dissociation energy for this molecule. For V_3^+, the measured predissociation threshold occurs 0.32 eV above the collision-induced dissociation (CID) measurement. Based in part on a theoretically suggested $^9A_2''$ ground state for V_3^+, it is suggested that predissociation of V_3^+ occurs efficiently only after the V ($3d\ ^4 4s^1$, $^6D_{1/2}$) + V_2^+ ($X\ ^4\Sigma_{g,1/2}^-$) separated fragment limit is exceeded in energy. Making a correction for the energy of this excited separated fragment limit then brings the photodissociation measurement into agreement with the CID result, and allows the bond energy to be determined as $D_0(V_2^+\text{–}V) = 2.323(1)$ eV. (Int J Mass Spectrom 204 (2001) 143–157) © 2001 Elsevier Science B.V.

Keywords: Bond energy; Dissociation energy; Predissociation

1. Introduction

The properties of small metal clusters are of considerable interest because of the potential uses of such species to catalyze specific chemical reactions. Many studies of the reactivity of small metal clusters have demonstrated that significant size-dependent differences in reactivity exist, and a more detailed understanding of the properties of these species is desirable. Toward this end, properties such as ionization potential [1–10], electron affinity and the development of band structure [11–17] dissociation energy [18–24], reaction rate [25–36], and adsorbate binding energetics and equilibria [37–48] have been measured for a number of small metal clusters and their ions. The ultimate aim of these studies is to understand the detailed chemistry of the small metal clusters, and to unify our understanding of these systems over the size range from small molecules to bulk crystalline metals. The research presented in this article contributes to this goal by increasing our knowledge of the smallest of these metal clusters, those containing only three atoms.

Spectra of the jet-cooled neutral transition metal dimers, recorded using the resonant two-photon ionization (R2PI) method, typically display clean, well-

* Corresponding author. E-mail: morse@chemistry.chem.utah.edu

1387-3806/01/$20.00 © 2001 Elsevier Science B.V. All rights reserved
PII S1387-3806(00)00331-6

resolved vibronic bands at low energies [49–63]. At sufficiently low energies, the observed spectral features may be organized into band systems, excited state vibrational levels may be assigned, and rotationally resolved studies may be used to measure bond lengths and deduce term symbols. As one proceeds to higher energies, however, the spectra of the open *d*-subshell transition metal dimers typically become more complicated, with electronic band systems overlapping with one another. At even higher energies, the density of vibronic states becomes so great that perturbations are rampant, and it can be difficult or impossible to make useful spectroscopic assignments. At still higher energies, the spectrum can become a near continuum, with vibronic densities of states approaching or exceeding 1 state/cm^{-1} [63–69].

For more than 25 examples, however, just when the information content in this spectroscopically "rich" quasicontinuum becomes nil, the R2PI spectrum abruptly ends [51,53,60,63,64,66,68–74]. Above a sharply defined energy, no further spectroscopic features are observed. This observed sudden break-off in spectral features clearly represents a predissociation threshold, with molecules excited above this threshold falling apart before they can be ionized and detected by the R2PI process. When the molecule under investigation has a sufficient density of states, the observed predissociation threshold coincides with the thermochemical dissociation threshold, so that accurate bond energies can be measured by this method. In many cases, the predissociation threshold can be located to an accuracy of a few wave numbers, implying that the measured bond energies are accurate to within approximately 1 meV. Table 1 presents a list of bond energies of metal dimers and trimers measured using this method. Bond energies measured by other methods are listed as well, for comparison.

Measurements of predissociation thresholds have also been used to estimate bond energies in previous investigations of gaseous transition metal ion complexes, such as $NiAr^+$ [75], $Ni^+ \cdot CO_2$ [76], $Ni^+ \cdot N_2O$ [77], $FeCH_2^+$ [78,79], $CoCH_2^+$ [78,79], $NiCH_2^+$ [79], $ScC_2H_2^+$ [80], $YC_2H_2^+$ [80], $LaC_2H_2^+$ [80], Co_2^+ [65,67], Ti_2^+ [67], V_2^+ [67], and Co_3^+ [67], and these methods have been extended to larger cluster ions, such as Ag_n^- ($n = 7 - 11$) [81], where the effects of finite fragmentation lifetimes must be factored into the analysis. Systems containing only a single metal atom tend to have a significantly reduced density of electronic states, making the assignment of a predissociation threshold to the thermochemical bond energy problematic in some cases. Likewise, for systems with significant fragmentation lifetimes, the need to estimate these lifetimes introduces an additional uncertainty into the analysis. Systems with two or three metal atoms, however, often have a sufficiently high density of electronic states and sufficiently rapid dissociation lifetimes for the bond energy to correspond directly to the measured predissociation threshold. In this article, we report the predissociation thresholds for $Al_3 \rightarrow Al_2 + Al$, $TiOMn^+ \rightarrow TiO^+ + Mn$, and $V_3^+ \rightarrow V_2^+ + V$, which are analyzed to obtain bond energies. Comparisons are made to other determinations of these bond energies when they are available.

2. Experimental

The bond energy of Al_3 reported in this article derives from an earlier publication from the Morse group in which a clear predissociation threshold was observed in the resonant two-photon ionization spectrum of Al_3 [82]. At that time, we did not recognize that this could be assigned to the lowest dissociation threshold of Al_3; nor did we recognize that the electronic band system that was observed originated from an electronically excited state of Al_3. A reexamination of these data now allows a strong conclusion to be drawn regarding the bond energy of Al_3. In the original study, Al_3 was produced using pulsed laser ablation of aluminum in the throat of a pulsed supersonic expansion of helium [82]. The jet-cooled molecules then passed through a skimmer into the extraction region of a Wiley-McLaren time-of-flight mass spectrometer [83] that was equipped with a reflectron for improved mass resolution [84–87]. The static voltages applied to the ion extraction lenses insured that any jet-cooled ions carried along in the

Table 1
Bond energies of metal dimers and trimers measured from predissociation thresholds[a]

Molecule	Number of valence electrons	Molecular ground state	Separated fragment limit [122]	Spin conservation possible?	Bond energy from predissociation (eV)	Bond energy (other methods)
Ti_2^+	7	[S = 1/2 likely]	$^3F + {}^4F$ S = 1/2, 3/2, 5/2	Yes	2.435(2) [67]	2.37(7) [21]
AlV	8	$^5\Delta_r$ or $^5\Sigma^+$[73]	$^2P^0 + {}^4F$ S = 1, 2	Yes	1.489(10) [73]	
TiZr	8	[$^3\Delta_r$ likely]	$^3F + {}^3F$ S = 0, 1, 2	Yes	2.183(1) [68]	
Zr_2	8	$^3\Delta_r$[123]	$^3F + {}^3F$ S = 0, 1, 2	Yes	3.052(1) [66]	
AlCr	9	$^6\Sigma^+$[73]	$^2P^0 + {}^7S$ S = 5/2, 7/2	Yes	2.272(9) [73]	
TiV	9	$^4\Sigma^-$[124]	$^3F + {}^4F$ S = 1/2, 3/2, 5/2	Yes	2.068(1) [64]	
V_2^+	9	$^4\Sigma_g^-$[116]	$^4F + {}^5$D S = 1/2, 3/2, 5/2, 7/2	Yes	3.140(2) [67]	3.13(14) [23]
TiNb	9	$^4\Sigma^-$[125]	$^3F + {}^6D$ S = 3/2, 5/2, 7/2	Yes	3.092(1) [68]	
ZrV	9	$^4\Sigma^-$[125]	$^3F + {}^4F$ S = 1/2, 3/2, 5/2	Yes	2.663(3) [68]	
V_2	10	$^3\Sigma_g^-$[50]	$^4F + {}^4F$ S = 0, 1, 2, 3	Yes	2.7526(1) [64]	2.49(13) [126] 2.47(22) [126]
VNb	10	$^3\Sigma^-$[57,58]	$^4F + {}^6D$ S = 1, 2, 3, 4	Yes	3.789(1) [58]	
NbCr	11	$^2\Delta_i$[63]	$^6D + {}^7S$ S = 1/2, 3/2, 5/2, 7/2, 9/2, 11/2	Yes	3.0263(6) [63]	
AlCo	12	$^3\Delta_i$[73]	$^2P^0 + {}^4F$ S = 1, 2	Yes	1.844(2) [73]	
YCo	12	[$^1\Sigma^+$ or $^3\Delta_i$ likely] [66]	$^2D + {}^4F$ S = 1,2	Perhaps	2.591(1) [66]	
Mo_2	12	$^1\Sigma_g^+$[127]	$^7S + {}^7S$ S = 0, 1, 2, 3, 4, 5, 6	Yes	4.476(10) [74]	4.18(22) [128]
AlNi	13	$^2\Delta_i$[72]	$^2P^0 + {}^3D$ S = 1/2, 3/2	Yes	2.29(5) [72]	
TiCo	13	$^2\Sigma^+$[129]	$^3F + {}^4F$ S = 1/2, 3/2, 5/2	Yes	2.401(1) [64]	
YNi	13	$^2\Sigma^+$[130]	$^2D + {}^3D$ S = 1/2, 3/2	Yes	2.904(1) [66]	
ZrCo	13	$^2\Sigma^+$[131]	$^3F + {}^4F$ S = 1/2, 3/2, 5/2	Yes	3.137(1) [66]	
ZrNi	14	[$^3\Delta_r$ or $^3\Sigma^-$ likely] [66]	$^3F + {}^3D$ S = 0, 1, 2	Yes	2.861(1) [66]	
NbCo	14	[$^3\Delta_r$ or $^3\Sigma^-$ likely] [66]	$^6D + {}^4F$ S = 1, 2, 3, 4	Yes	2.729(1) [66]	
VNi	15	$^4\Sigma^-$[124]	$^4F + {}^3D$ S = 1/2, 3/2, 5/2	Yes	2.100(1) [64]	
NbNi	15	$^4\Sigma^-$[132]	$^6D + {}^3D$ S = 3/2, 5/2, 7/2	Yes	2.780(1) [66]	
Co_2^+	17	[S = 1/2, 3/2, or 5/2 likely]	$^4F + {}^3F$ S = 1/2, 3/2, 5/2	Yes	2.765(1) [65,67]	2.75(10) [133]

(continued on next page)

Table 1 *(continued)*

Molecule	Number of valence electrons	Molecular ground state	Separated fragment limit [122]	Spin conservation possible?	Bond energy from predissociation (eV)	Bond energy (other methods)
Rh_2	18	$^5\Delta_g$[134]	$^4F + {}^4F$ $S = 0, 1, 2, 3$	Yes	2.4059(5) [69]	2.84(26) [135] 2.92(22) [136] 1.4(3) [137]
Ni_2^+	19	[S = 1/2 or 3/2 likely]	$^3D + {}^2D$ $S = 1/2, 3/2$	Yes	2.32(2) [120]	2.08(7) [121] 2.245(25) [60]
Ni_2	20	S = 0, 1 strongly mixed [60,138,139]	$^3D + {}^3D$ $S = 0, 1, 2$	Yes	2.042(2) [60]	2.03(30) [140] 2.36(22) [140]
NiPt	20	[S = 0, 1 strongly mixed]	$^3D + {}^3D$ $S = 0, 1, 2$	Yes	2.798(3) [53]	
Pt_2	20	S = 0, 1 strongly mixed [141]	$^3D + {}^3D$ $S = 0, 1, 2$	Yes	3.141(3) [51]	3.71(61) [142] 3.71(16) [142]
Co_3^+	26	unknown	unknown	unknown	2.086(2) [67]	2.04(13) [24]

[a] References are provided in square brackets throughout. Molecular ground states that are conjectured, without either experimental or calculational support are given in square brackets as well.

molecular beam were diverted so that they did not strike the detector. Within the Wiley-McLaren extraction assembly, the molecular beam was exposed to the pulsed output radiation of a Nd:YAG-pumped dye laser, which was followed by a pulse of excimer laser radiation generated from a KrF gas mixture. Ions produced by the resonant two-photon ionization process traversed a time-of-flight mass spectrometer and impacted on a microchannel plate detector. The resulting ion signal was preamplified, digitized, and processed using a DEC LSI-11 microcomputer. By monitoring the ion signal at mass 81 as the dye laser was scanned, an optical spectrum of Al_3 was recorded. The dye laser employed for these experiments was calibrated using the two-photon $3s^24p^1$, $^2P^0_{1/2,3/2} \leftarrow 3s^23p^1$, $^2P^0_{1/2,3/2}$ atomic aluminum transitions, which occur in the 16 400–16 500 cm^{-1} range, and the frequency of the observed dissociation threshold at 19 378 cm^{-1} is thought to be accurate to ± 10 cm^{-1}.

The photodissociation experiments on $TiOMn^+$ and V_3^+ employed a jet-cooled ion photodissociation instrument that was described in our previous studies of the photodissociation of Ti_2^+, V_2^+, Co_2^+, and Co_3^+ [65,67]. Briefly, the output radiation of a pulsed KrF excimer laser (248 nm, ~20 mJ/pulse) was focused onto a rotating and translating metal target disk, which was placed in the throat of a pulsed supersonic expansion of helium (~10 psig). The resulting metal plasma was swept through a clustering region 2 mm in diameter and approximately 3 cm in length before expanding supersonically into vacuum (10^{-4} Torr). The molecular beam was skimmed and admitted into a differentially pumped chamber, where a pulsed Wiley-McLaren assembly extracted the jet-cooled ions at right angles to the supersonic beam [83]. The Wiley-McLaren lenses also provided the aperture required for another stage of differential pumping. Einzel lenses were then used to bring the ion packet to a longitudinal and radial focus 1.73 m downstream of the extraction point, in a third chamber that was maintained at a pressure of $\sim 9 \times 10^{-7}$ Torr. Here the pulsed output radiation of an excimer-pumped dye laser crossed the ion beam at right angles, timed to coincide with the arrival of the ion of interest in the chamber.

Following the exposure of the ions to this pulsed radiation, the ions entered a reflecting electric field, which could be set to a voltage that would transmit parent ions but reflect the fragmentation products. The reflected fragmentation products were then detected using a microchannel plate detector connected to a 40 MHz digital oscilloscope. Analysis of the dependence of the photofragment signal on the potential applied to the electrostatic reflector permitted the ratio of the parent to fragment masses to be determined unambiguously. Thus, the timing of the photofragmentation

laser determined the parent ion that was investigated and the voltage dependence of the photofragment signal allowed the identity of the fragment ion to be determined as well.

The predissociation threshold of $TiOMn^+$ was calibrated by directing some of the dye laser radiation through a heated I_2 absorption cell, and the resulting absorption lines were correlated with the I_2 absorption atlas of Gerstenkorn and Luc [88]. The predissociation threshold observed for V_3^+, however, fell outside the range of the I_2 atlas. This problem was overcome by Raman shifting the dye laser radiation in high pressure H_2 (≈500 psi). The stimulated Raman scattering which results from this process occurs only on the $Q(1)$ line, leading to a precise shift of the laser wave number by 4155.163 cm^{-1} at 500 psi [89]. The I_2 calibration spectrum was then recorded using the first Stokes radiation emerging from the Raman cell, and calibration was again accomplished by correlating the absorption lines with the I_2 atlas [90,91]. Because the dye laser radiation intersected the ion beam at right angles, no Doppler correction was required.

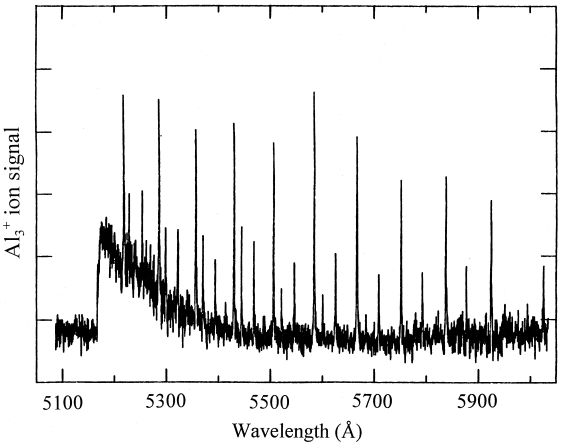

Fig. 1. Resonant two-photon ionization spectrum of Al_3, obtained by scanning a dye laser over the 510–600 nm range for the excitation photon, and using a KrF excimer laser for the ionization photon. A discrete band system is observed along with a continuous absorption that grows in intensity toward the blue. A sharp dissociation threshold is observed at 5160 Å (19 378 ± 10 cm^{-1}). This is used to establish the bond energy of Al_3 as $D_0(Al_2–Al)$ = 2.701 ± 0.005 eV as described in the text. Note that the energy increases as one moves to the left. (Used with permission from [82])

3. Results

3.1. Bond energy of Al_2–Al

In our previous investigation of Al_3, a weak band system was observed in the range 516–602 nm [82]. This band system, exhibited in Fig. 1, displays an extended progression in a vibrational mode of the upper state with a vibrational frequency of 273 cm^{-1}. A second upper state vibrational mode with a frequency of 205 cm^{-1} is observed in combination with the main progression. Finally, one lower state vibrational mode is evident in the spectrum as hot bands displaced 133 cm^{-1} to the red of the corresponding members of the main progression.

In addition to the discrete band system, a continuous absorption grows in toward shorter wavelengths, terminating abruptly at 5160.5 ± 2.7 Å (19 378 ± 10 cm^{-1}). The observation of a continuous absorption is unusual for a jet-cooled triatomic molecule, and is indicative of a high density of accessible vibronic states in this energy range. Moreover, the discrete absorption features display a lifetime that is identical, within experimental error, to that of the underlying continuum, suggesting that there is substantial coupling between the discrete electronic state and the upper state of the continuous absorption, as has been discussed previously [82]. The excited state lifetime in the continuum has been measured to fall in the range of 24–35 μs, while any excited states lying above the continuum edge must decay in less than 10 ns or they would be detected in these experiments. The abrupt drop in excited state lifetime clearly indicates the onset of predissociation in this dense manifold of vibronic levels.

After our initial work on Al_3 was published [82], a negative ion photoelectron spectroscopic study of Al_3^- was completed by Villalta [92]. The vibrational frequencies of the neutral Al_3 ground state were measured to be 235 ± 15 and 360 ± 15 cm^{-1}, proving that the lower state of the transition displayed in Fig. 1 is not the ground state. This conclusion was reached because the hot band frequency found for the spec-

trum of Fig. 1 was 133 cm^{-1}, not 235 or 360 cm^{-1}. A low-lying excited state of Al_3, with a 0−0 excitation energy of 2404 ± 40 cm^{-1}, however, was determined to have vibrational frequencies of 135 ± 15 and 305 ± 15 cm^{-1}, making it the likely lower state for the band system displayed in Fig. 1 [92].

Theoretical studies [93], in combination with the photoelectron experiments [92], have now established that the ground state of Al_3 is a $^2A_1'$ state of D_{3h} symmetry, with a $^2A_2''$ state (also of D_{3h} symmetry) lying 1550 cm^{-1} above. A low-lying $^4E''$ (in D_{3h}) state has also been calculated by a number of investigators [93–98], and was thought to be a candidate for the ground state for several years. This state undergoes Jahn-Teller distortion to form a $^4A_2$ and $^4B_1$ pair of states in C_{2v} symmetry. It is now well-established that the $^4A_2$ state gives the minimum energy geometry, whereas the $^4B_1$ state provides the saddle point connecting equivalent $^4A_2$ minima [93,94,96,98]. In the most detailed calculation to date, the $^4A_2$ state is calculated to lie at 1725 cm^{-1}, and to have vibrational modes with frequencies of 320 cm^{-1} and 153 cm^{-1} [93]. This strongly suggests that the $^4A_2$ state is the state observed by photoelectron spectroscopy at 2404 cm^{-1}, with vibrational frequencies of 305 and 135 cm^{-1}. It also suggests that it is the lower state that is responsible for the band system displayed in Fig. 1, because this lower state has one vibrational mode with a vibrational interval of 133 cm^{-1}.

In retrospect, it is perfectly plausible that the lower level of the band system displayed in Fig. 1 could be a metastable excited state, particularly the lowest energy quartet state of Al_3. This spectrum was quite weak in intensity, and all efforts to increase its intensity by increasing the concentration of Al_3 only led to a drop in signal. At the time, it was thought that lengthening the amount of time that the aluminum clusters spent in the high-pressure zone prior to expansion caused the Al_3 concentration to be depleted by the formation of larger clusters. It now seems likely that the increased time spent in the high-pressure zone instead led to a more effective quenching of the metastable $^4A_2$ state of Al_3.

As was discussed in our previous article on this molecule [82], both the continuous absorption and the discrete transitions displayed in Fig. 1 cease at the same energy, given by 19 378 ± 10 cm^{-1}. Thus, both absorptions must arise from the same lower state of the molecule, since both have the same predissociation threshold. In our previous study, we assumed that this was the ground state, and suggested that the bond energy, $D_0(Al_2–Al)$, was given by the energy of the predissociation threshold as $D_0(Al_2–Al)$ = 19 378 ± 10 cm^{-1} (2.403 ± 0.001 eV) [82]. With the assignment of the lower level of our band system as the $^4A_2$ state, which is measured to lie 2404 ± 40 cm^{-1} above the ground state [92], the bond energy must be revised to a value of $D_0(Al_2–Al)$ = 21 782 ± 42 cm^{-1} (2.701 ± 0.005 eV). This assumes that there is no barrier to dissociation to ground state fragments, which are now known to consist of Al_2 ($X\ ^3\Pi_u$) + Al ($^2P^o$) [99–102].

In general, one expects no problems in correlating an S = 3/2 state to these separated fragments, since an S = 3/2 state is readily generated from $^3\Pi_u$ + $^2P^o$. More explicitly, consideration of the molecular states that are formed when the $^2P^o$ atom approaches the $^3\Pi_u$ dimer along a path that preserves C_{2v} symmetry will allow us to deduce whether the excited quartet state accessed in the spectrum shown in Fig. 1 can correlate to ground state separated fragments. Again no problems arise, since under C_{2v} the $X\ ^3\Pi_u$ state of Al_2 is resolved into $^3A_1 \oplus {}^3B_1$ and the $^2P^o$ state of atomic Al is resolved into $^2A_1 \oplus {}^2B_1 \oplus {}^2B_2$. The direct product of these two sets then generates all of the states deriving from the $^3\Pi_u$ + $^2P^o$ separated fragment limit. From this analysis, we find that the C_{2v} states that correlate to ground state separated fragments include $^2A_1$ (2 states), $^2A_2$, $^2B_1$ (2 states), $^2B_2$, $^4A_1$ (2 states), $^4A_2$, $^4B_1$ (2 states), and $^4B_2$. Thus, the S = 1/2 and S = 3/2 states that are possible under C_{2v} symmetry can correlate to the ground separated fragment limit. On this basis we conclude that there are no symmetry-required barriers to dissociation. The sharpness of the observed threshold then argues for dissociation at the thermochemical threshold, and we therefore assign the dissociation energy of Al_3 as $D_0(Al_2–Al)$ = 2.701 ± 0.005 eV.

The value of $D_0(Al_2–Al)$ determined here is considerably higher than previous estimates, regardless of whether they are based on theory or experiment. Early

ab initio estimates of $D_0(Al_2–Al)$ have fallen in the range 1.55–1.93 eV [94,96,103]. Even a high quality 1998 coupled-cluster single double triple [CCSD(T)] correlation calculation, a level of theory that is generally in good agreement with spectroscopic experiments, yielded an estimate of only 2.24 eV for $D_0(Al_2–Al)$ [93]. The ability of theoretical calculations to treat systems with fewer electrons more accurately tends to lead to an underestimation of bond energies. This accounts for the low bond energies found in the early calculations. The coupled-cluster method, however, is a size-consistent procedure that should provide more accurate estimates of dissociation energies than the other methods [104]. This is clearly reflected in the higher bond energy calculated for Al_3 using this technique. It is surprising that this state-of-the-art calculation has failed to recover the full dissociation energy, however.

On the experimental side, a collision-induced dissociation measurement of the bond energy of Al_3^+ yielded $D_0(Al_2^+–Al) = 1.12 \pm 0.35$ eV [105]. Combining this result with the ionization energies $IE(Al_2) = 5.989 \pm 0.002$ eV [106] and $IE(Al_3)=6.46 \pm 0.04$ eV [29] using the thermochemical cycle

$$D_0(Al_2 - Al) = D_0(Al_2^+ - Al) + IE(Al_3) - IE(Al_2) \quad (1)$$

then gives $D_0(Al_2–Al) = 1.59 \pm 0.35$ eV. This value is comparable to the lowest of the theoretical calculations, and is almost certainly too low. This is presumably due to insufficient collisional cooling, leading to vibrationally hot Al_3^+ ions. In a recent conversation with Professor Scott Anderson on this topic, he stated that this value is possibly too low, and is almost certainly not too high [107]. A 1989 photodissociation study of Al_3^+, confirms this possibility, with photodissociation of Al_3^+ occurring at wavelengths below 580 nm, corresponding to energies above 2.14 eV [108]. Again, however, this study may have been hampered by incomplete collisional cooling of the Al_3^+ ions. Although weak signal persists in the photodissociation spectrum of Al_3^+ down to about 600 nm, a sharp increase in signal for the $Al_3^+ \rightarrow Al_2^+ + Al$ process occurs near 550 nm [108].

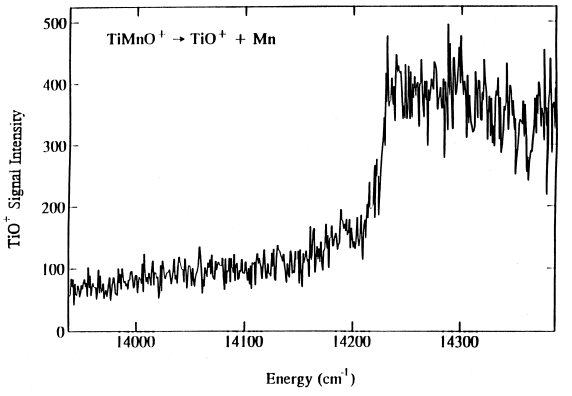

Fig. 2. Predissociation threshold of $TiOMn^+$, corresponding to dissociation into $TiO^+ + Mn$. This was measured by intersecting a beam of jet-cooled $TiOMn^+$ ions with the output of a dye laser and monitoring the production of TiO^+ ions. From the observed predissociation threshold at 14219 cm^{-1}, a bond energy of $D_0(TiO^+–Mn)=1.763 \pm 0.001$ eV is derived. Note that the energy increases as one moves to the right.

This sharp increase leads to an approximate doubling of the fragmentation signal, but occurs in a portion of the photodissociation spectrum where the absorption cross section is quite small. Assuming that the weaker signal that persists to longer wavelengths is due to hot Al_3^+ ions, the increase in photodissociation signal that occurs at 550 nm converts to a bond energy of $D_0(Al_2^+–Al) = 2.25$ eV. Application of the thermochemical cycle (1) then gives $D_0(Al_2–Al) = 2.73$ eV, in excellent agreement with the results of the present study.

3.2. Bond energy of TiO^+–Mn

In an effort to make a photodissociation measurement of the bond energy of Mn_2^+, a TiMn alloy sample was used in the ion photodissociation instrument. Although no signal was observed for Mn_2^+, a strong ion signal was observed at mass 119 due to the $TiOMn^+$ cation, which was produced without an intentional source of oxygen. A predissociation threshold was observed for this species at 14 219 $\pm$ 8 cm^{-1} (1.763 $\pm$ 0.001 eV), as displayed in Fig. 2. The fragment ion formed in the dissociation process was determined to be TiO^+ by varying the voltages of the reflecting electric field. This test showed maximum

fragment signal when the voltages were adjusted to the predicted values for the process

$$TiOMn^+ \rightarrow TiO^+ + Mn, \quad (2)$$

and reduced or negligible signal when the voltages were adjusted to those required for the other possible fragmentation pathways

$$TiOMn^+ \rightarrow TiO + Mn^+ \quad (3)$$

$$TiOMn^+ \rightarrow Ti^+ + MnO \quad (4)$$

$$TiOMn^+ \rightarrow Ti + MnO^+ \quad (5)$$

This is as expected, because the thermochemical cycles

$$D_0(TiO^+ - Mn) - D_0(TiO - Mn^+) = IE(TiO) - IE(Mn) \quad (6)$$

$$D_0(TiO^+ - MnO) - D_0(Ti - MnO^+) = IE(Ti) - IE(MnO) \quad (7)$$

$$D_0(TiO^+ - Mn) - D_0(Ti^+ - OMn) = D_0(MnO) - D_0(Ti^+ - O) \quad (8)$$

when combined with the values of IE(TiO) = 6.8197(7) eV [109], IE(Mn) = 7.4367 eV [110], IE(Ti) = 6.8281 eV [111], IE(MnO) = 8.30 ± 0.15 eV [112], D_0(MnO) = 3.82 ± 0.08 eV [113], and $D_0(Ti^+–O)$ = 6.88 ± 0.07 eV [114], demonstrate that processes (3)–(5) require 0.617, 3.06 ± 0.11, and 4.53 ± 0.19 eV, respectively, more energy than process (2). Thus, the fragmentation process observed produces the lowest energy products, as expected. The bond energy is assigned as the photon energy at the predissociation threshold, giving $D_0(TiO^+–Mn)$ = 1.763 ± 0.001 eV. The thermochemical cycles (6)–(8) then provide $D_0(TiO–Mn^+)$ = 2.380 ± 0.001 eV, $D_0(Ti^+–OMn)$ = 4.82 ± 0.11 eV, and $D_0(Ti–OMn^+)$ = 6.29 ± 0.18 eV.

3.3. Bond energy of V_2^+–V

Fig. 3 displays the photofragmentation spectrum of V_3^+, as obtained with the reflecting electric field set to detect the V_2^+ fragment. A predissociation threshold is observed at 20 852 ± 8 cm^{-1} (2.585 ± 0.001 eV), where it rises out of a fairly high background signal that continues to frequencies below the threshold. A small portion of this background signal comes from collision-induced dissociation processes due to the background gas in the instrument. This is present even when the photodissociation laser is blocked. Most of the background signal, however, is induced by the dye laser radiation. Because the background signal is mostly photoinduced, a scan to longer wavelengths was attempted in an effort to observe a second dissociation threshold. A gradual decrease in fragmentation yield was observed, without another sharp threshold. Attempts to reduce the dye laser-induced background signal beyond that observed in Fig. 3 by decreasing the fluence of the dye laser were not successful, leading only to a reduction in overall signal intensity.

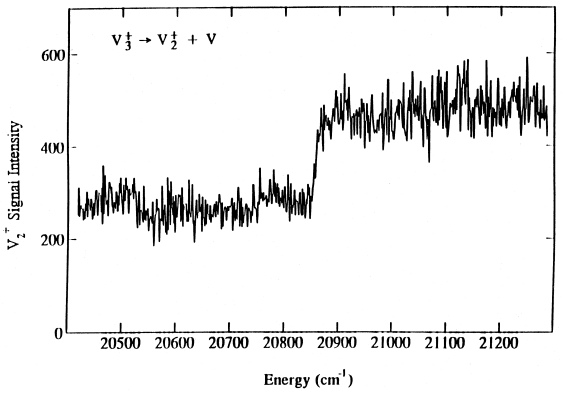

Fig. 3. Predissociation threshold of V_3^+, corresponding to dissociation into V_2^+ + V. Again, this was measured by intersecting a beam of jet-cooled V_3^+ ions with the output of a dye laser and monitoring the production of V_2^+ ions. As discussed in the text, the observed predissociation onset is assigned to the threshold for production of V_2^+ ($X\ ^4\Sigma_g^-$, Ω = 1/2)+V ($3d^44s^1$, $^6D_{1/2}$). This leads to a bond energy of $D_0(V_2^+–V)$ = 2.323 ± 0.001 eV. Note that the energy increases as one moves to the right.

Based on the spectrum displayed in Fig. 3, we are tempted to assign the bond energy of V_3^+ as $D_0(V_2^+–V)$ = 20 852 ± 8 cm^{-1} (2.585 ± 0.001 eV). This value differs substantially from a CID measurement of $D_0(V_2^+–V)$ = 2.27 ± 0.09 eV, however [23]. The 0.32 ± 0.09 eV difference between these measure-

ments contrasts with what has been found for Ti_2^+, V_2^+, Co_2^+, and Co_3^+ [65,67], where photodissociation and CID measurements of bond energies have agreed to within the quoted error limits (see Table 1). The discrepancy in the case of V_3^+ is therefore unexpected and suggests that a systematic error may be present in one or both experiments, or in their interpretation.

If the error lies in the CID experiment, it likely originates from a sample of V_3^+ ions that retains an unexpectedly large amount of internal energy. This would make the bond energy measured in the CID experiments lower than that measured by photodissociation, as observed. Although the CID experiments conducted in the Armentrout group employ a supersonic expansion to cool the internal degrees of freedom and the analysis explicitly considers the thermal energy content on the ions, it may be seen from Table 1 that bond energies measured by this technique are slightly lower than those found by photodissociation experiments for Ti_2^+, V_2^+, Co_2^+, and Co_3^+. The differences are quite small, however, ranging from 0.01 to 0.065 eV, and none of them creates a discrepancy that lies outside of the quoted error limits. Although these small differences may indicate that colder ions are generated in the photodissociation instrument, it is hard to understand why V_3^+ should be significantly more difficult to cool than V_2^+ or Co_3^+, for example. Attempts to fit the CID data to a bond energy that is constrained to the value of the photodissociation measurement have not been successful. The difference between the CID measurement of the bond energy and the sharp predissociation threshold found in the photodissociation experiment is real.

If the error lies in the photodissociation experiment and the true dissociation threshold lies 0.32 eV lower than that observed in Fig. 3, this could explain the presence of a significant photodissociation signal to the red of the measured threshold. However, a search for a second threshold within the range expected from the CID measurement was fruitless. Further, the dissociation threshold observed in Fig. 3 is real and reproducible, and if it does not represent the true bond energy, it still requires a plausible explanation. One possibility is that the photoexcited states of V_3^+ do not efficiently predissociate until a particular excited fragment limit is reached. In this connection, it should be noted that the discrepancy between the two measured values, 0.32 ± 0.09 eV (2540 ± 725 cm^{-1}), encompasses the range of energies required to excite a ground state ($3d^34s^2$, $^4F_{3/2}$) vanadium atom to the $3d^44s^1$, ^6D_J states, which lie 2112.32–2424.89 cm^{-1} above ground state atoms [115]. The possibility that photoexcited V_3^+ could efficiently dissociate to V ($3d^44s^1$, ^6D) + V_2^+ ($X\,^4\Sigma_g^-$) [116] but not to V ($3d^34s^2$, ^4F) + V_2^+ ($X\,^4\Sigma_g^-$) would therefore reconcile the two experiments.

Little is known about the ground or excited electronic states of V_3^+. However, an early investigation of the transition metal trimers by Walch and Bauschlicher has suggested that V_3^+ has a $^9A_2''$ ground state in a D_{3h} geometry [117,118]. This state derives from an electronic configuration of

$$(4sa_1')^2(3d\sigma a_1')^2(3d\pi'' a_2'')^2(3d\pi' e')^2(3d\delta' a_1')^1 \cdot (3d\delta' e')^2(3d\delta'' a_1'')^1(3d\delta'' e'')^2 \quad (9)$$

in which the $4sa_1'$ orbital is a symmetric linear combination of the three atomic 4*s* orbitals and the 3*d*-based molecular orbitals are identified as σ, π, or δ based on a local *z* axis which is taken to point toward the center of the molecule, which is equilateral triangular in shape. The $4sa_1'$, $3d\sigma a_1'$, and $3d\pi'' a_2''$ orbitals are all strongly bonding in character, whereas the $3d\pi' e'$ orbital possesses some bonding character. The $3d\delta' a_1'$, $3d\delta' e'$, $3d\delta'' a_1''$, and $3d\delta'' e''$ orbitals are essentially nonbonding in character [117,118]. The existence of so many orbitals with little bonding character is essential for the formation of the proposed high-spin $^9A_2''$ ground state, because it is the near-degeneracy of these orbitals that favors the formation of a high-spin ground state.

If the ground state of V_3^+ is the $^9A_2''$ state proposed by Walch and Bauschlicher [117,118], then excitations that are allowed under electric dipole selection rules would populate excited electronic states that also have $S = 4$. Assuming that spin is a good quantum number in V_3^+, such $S = 4$ states cannot dissociate at the ground separated fragment limit, because $S=4$ cannot be generated by the combination of a ground state vanadium atom ($3d^34s^2$, ^4F) with the known

ground state of V_2^+ ($X\,^4\Sigma_g^-$) [116]. Only states with $S = 0$, 1, 2, or 3 derive from the ground separated fragment limit. On the other hand, excited states of V_3^+ with $S = 4$ should predissociate efficiently to V ($3d^4 4s^1$, ^6D) + V_2^+ ($X\,^4\Sigma_g^-$), because this separated fragment limit generates states of the V_3^+ ion with $S =$ 1, 2, 3, and 4. Thus, $S = 4$ states can dissociate at this limit while preserving the value of S. At energies below the V ($3d^4 4s^1$, ^6D) + V_2^+ ($X\,^4\Sigma_g^-$) separated fragment limit, predissociation can still occur, but it is expected to proceed at a lower rate because it requires spin-orbit coupling between the $S = 4$ state that is initially excited and an $S = 3$ state that can predissociate at the ground state separated fragment limit.

Assuming that the predissociation limit observed in Fig. 3 at 20 852 ± 8 cm^{-1} corresponds to the first separated fragment limit that can generate an $S = 4$ state of the trimer, this is the V ($3d^4 4s^1$, $^6D_{1/2}$)+V_2^+ ($X\,^4\Sigma_{g,1/2}^-$) limit, which lies 2112.32 cm^{-1} above ground state fragments [115]. This places the true value of $D_0(V_2^+–V)$ at 18 740 ± 8 cm^{-1} (2.323 ± 0.001 eV), a value that is now in good agreement with the CID measurement of 2.27 ± 0.09 eV. The slightly larger value of $D_0(V_2^+–V)$ obtained by way of photodissociation measurement is now in line with the differences previously measured for Ti_2^+, V_2^+, Co_2^+, and Co_3^+, and may result from improved supersonic cooling in the ion photodissociation instrument. On the basis of the agreement between these values, the theoretical evidence for a high-spin $^9A_2''$ ground state for V_3^+, and the photoinduced background signal lying to the red of the sharp predissociation threshold in Fig. 3, we believe that 18 740 ± 8 cm^{-1} (2.323 ± 0.001 eV) represents the true value of $D_0(V_2^+–V)$.

This may be combined with the known ionization energies of V_2 (IE = 51 271.14 ± 0.5 cm^{-1}) [116] and V_3 (IE = 44 342 ± 3 cm^{-1}) [119] using the thermochemical cycle

$$D(V_2 - V) = D_0(V_2^+ - V) + IE(V_3) - IE(V_2) \quad (10)$$

to obtain the bond energy of the neutral V_3 molecule as $D_0(V_2–V)$ = 11 811 ± 9 cm^{-1} (1.464 ± 0.001 eV). Likewise, our value may be combined with the ionization energies of V (IE = 54 411.67 ± 0.17 cm^{-1}) [58] and V_2 (IE = 51 271.14 ± 0.5 cm^{-1}) [116] using the thermochemical cycle

$$D_0(V_2 - V^+) = D_0(V_2^+ - V) - IE(V_2) + IE(V) \quad (11)$$

to obtain $D_0(V_2–V^+)$ = 21 881 ± 9 cm^{-1} (2.713 ± 0.001 eV). Finally, the atomization energies (AE) of V_3 and V_3^+ may be readily calculated using the bond energies of V_2 (D_0 = 22 201 ± 1 cm^{-1}) [64,71] and V_2^+ (D_0 = 25 341.6 ± 1.1 cm^{-1}) [67,69] and the thermochemical cycles

$$AE(V_3) = D_0(V_2 - V) + D_0(V_2) \quad (12)$$

$$AE(V_3^+) = D_0(V_2^+ - V) + D_0(V_2^+) \quad (13)$$

to give $AE(V_3)$ = 34012 ± 9 cm^{-1} (4.217 ± 0.001 eV) and $AE(V_3^+)$ = 44 082 ± 9 cm^{-1} (5.465 ± 0.001 eV).

4. Discussion

In this article, we report three bond energies, all measured by the onset of predissociation in a dense vibronic spectrum. For one of the molecules, Al_3, the spectrum arises from an electronically excited $^4A_2$ state of Al_3, and the dissociation energy is higher than the measured predissociation limit by the energy of the metastable $^4A_2$ state. For another of the molecules, V_3^+, it is suggested that dynamical constraints (spin conservation) prevent the molecule from efficiently dissociating at the ground separated fragment limit, so that the measured predissociation threshold must be reduced by the energy of the excited separated fragment asymptote. For the third example, $TiOMn^+$, it is suggested that the measured predissociation threshold provides the true bond energy of the molecule.

The fact that only one of the three predissociation thresholds is thought to correspond to the true bond energy, while the others must be increased by 2404 cm^{-1} (for Al_3) and decreased by 2112.32 cm^{-1} (for V_3^+) is troubling. If less were known about the electronic states of Al_3 or if the bond energy of V_3^+ had not been measured by another method prior to this

investigation, these studies would have led to erroneous values of the corresponding bond energies.

With this in mind, we have reconsidered the bond energies measured by predissociation methods as listed in Table 1, to establish which, if any, of these may require correction. All of the molecules listed in the table contain transition metals, and it is our experience that metal dimers containing one or two transition metal atoms are generally effectively cooled to their lowest spin-orbit states in a supersonic expansion of helium. Unlike the example of Al_3, we do not generally expect metastable electronic states to be populated in experiments on jet-cooled transition metal dimers. Exceptions include Ni_2, where the compact nature of the 3*d* orbitals makes electronic cooling quite difficult using helium carrier gas [60], and Mo_2, where the low density of electronic states arising from the ground separated atom limit of $4d^5 5s^1$, $^7S + 4d^5 5s^1$, ^7S makes the metastable $^3\Sigma_u^+$, $^5\Sigma_g^+$, etc. states difficult to cool [74]. In these examples, however, these problems are well understood and there are no errors arising from these effects in the values listed in Table 1. Incomplete collisional cooling could also be a problem for Ni_2^+, again due to the small size of the partially occupied 3*d* orbitals and their resultant shielding by the remaining electrons in the molecule, but this effect would make the measurement of $D_0(Ni_2^+)$ artificially low. The value of $D_0(Ni_2^+)$ measured by photodissociation methods (2.32 ± 0.02 eV) [120] is actually larger than that measured by collision-induced dissociation methods (2.08 ± 0.07 eV) [121], indicating that metastable electronic states are more of a potential problem in the CID measurement than in the photodissociation measurement.

The possibility that total electron spin could be retained as a good quantum number in a molecule as complicated as V_3^+ is surprising, because the expected density of electronic states is very large, and spin-orbit interaction in vanadium clusters is not negligible. Nevertheless, the available evidence suggests that predissociation along a spin-forbidden pathway is slowed significantly. In light of this possibility, it is appropriate to reconsider the predissociations of all of the molecules listed in Table 1. If the ground electronic state of the molecule has a value of *S* that cannot correlate to the ground separated fragment limit, as we believe occurs for V_3^+, then it is possible that the predissociation threshold corresponds to an excited separated fragment limit, making it higher than the true bond energy by the excitation energy of the separated fragments. To investigate this possibility, we have included in Table 1 the known or predicted ground electronic state symmetries of all of the molecules listed, along with the ground separated fragment limits and the resultant values of *S*. In all cases except for YCo and Co_3^+, it is definite that spin can be conserved in the predissociation process. Thus, it appears that the bond energies deduced from the abrupt onset of predissociation in a dense set of vibronic energy levels are probably valid for most of these molecules.

In the case of YCo, we have previously argued that the ground state is more likely to be an $s\sigma^2 d\pi^4 d\sigma^2 d\delta^3 s\sigma^{*1}$, $^3\Delta_i$ state than a $s\sigma^2 d\pi^4 d\sigma^2 d\delta^4$, $^1\Sigma^+$ state [66]. If this prediction holds true, then *S* can be conserved throughout the excitation and predissociation process, and our value of $D_0(YCo) = 2.591 \pm 0.001$ eV remains valid. On the other hand, if the ground state is a $^1\Sigma^+$ state and *S* is conserved throughout the process, our quoted bond energy for this molecule will require revision. Further experiments or theoretical calculations will be required to establish the facts unequivocally.

In the case of Co_3^+, almost nothing is known about the ground electronic state. The same is true of the Co_2^+ fragment. For the dissociation energy of Co_3^+, however, an independent value of the bond energy, obtained by CID methods [24], agrees with the predissociation threshold measurement [67] to an accuracy of 0.046 eV. This is well within the error limits (±0.13 eV) quoted for the CID measurement [24], and demonstrates that spin conservation presents no problems in the photodissociation of Co_3^+. It appears that the example of V_3^+ is truly anomalous, in that it is the only example currently known of a transition metal cluster in which spin conservation interferes with the measurement of a bond energy by the observation of a predissociation threshold.

This study has highlighted the importance of hav-

ing several tools at our disposal as we study the complicated metal molecules. Without the ab initio calculations and negative ion photoelectron spectra for Al_3, our observation of a predissociation threshold would have led to an erroneous conclusion. Likewise, without the CID study of V_3^+, our observed photodissociation threshold would again have led to a wrong conclusion. Continued progress in understanding the electronic structure, chemical bonding, and chemical reactions of small metal molecules is a synergistic endeavor, in which all of the facts gleaned about a particular molecule, by all of the available methods, must be sorted out, analyzed, and rebuilt into a coherent whole. When this is done, a highly detailed and satisfying picture of these important and complicated species begins to emerge.

5. Conclusion

Predissociation thresholds have been observed in the resonant two-photon ionization spectrum of Al_3 and in the photodissociation spectra of $TiOMn^+$ and V_3^+. The predissociation threshold in Al_3 is shown to occur in an absorption system that originates from a metastable, excited $^4A_2$ state (in the C_{2v} point group), and the energy of this $^4A_2$ state is added to the observed threshold to provide the bond energy of Al_3 as $D_0(Al_2–Al) = 2.701(5)$ eV.

For V_3^+, a sharp predissociation threshold is also observed, but it lies within a weaker dissociation continuum that is induced by absorption of dye laser radiation to the red of the observed threshold. In addition, the observed predissociation threshold is significantly larger than the bond energy of V_3^+ measured by CID methods. These experiments may be reconciled if the ground electronic state of V_3^+ is a $^9A_2''$ state, as has been suggested in a theoretical study of the 3*d* transition metal trimers, provided that the total electronic spin remains a nearly good quantum number in the V_3^+ system. This possibility explains how a nonzero photodissociation yield may be observed to the red of the predissociation threshold, while also explaining the significant increase in fragmentation yield when the V_2^+, $X\ ^4\Sigma_g^-$ + V, $3d^4 4s^1$, ^6D excited separated fragment limit is exceeded in energy. Making a correction for the energy of the V, $3d\ ^4 4s^1$, $^6D_{1/2}$ state then provides $D_0(V_2^+–V) = 2.323 \pm 0.001$ eV. This may be combined with literature values of other properties to give $D_0(V_2–V) = 1.464 \pm 0.001$ eV, $D_0(V_2–V^+) = 2.713 \pm 0.001$ eV, and the atomization energies $AE(V_3) = 4.217 \pm 0.001$ eV and $AE(V_3^+) = 5.465 \pm 0.001$ eV.

A predissociation threshold is also observed in the spectrum of $TiOMn^+$, corresponding to dissociation to TiO^+ + Mn. There is no evidence to suggest that this arises from a metastable excited state of $TiOMn^+$ or that dissociation to the ground separated fragments is spin-forbidden. In the absence of other information, the bond energy $D_0(TiO^+–Mn)$ is set equal to the observed predissociation threshold, giving $D_0(TiO^+–Mn) = 1.763 \pm 0.001$ eV. Thermochemical cycles then provide $D_0(TiO–Mn^+) = 2.380 \pm 0.001$ eV, $D_0(Ti^+–OMn) = 4.82 \pm 0.11$ eV, and $D_0(Ti–OMn^+) = 6.29 \pm 0.18$ eV.

Acknowledgements

The authors thank the National Science Foundation for support of this research under grant no. CHE-9626557. Acknowledgment is also made to the donors of the Petroleum Research Fund, administered by the American Chemical Society for partial support of this work, and to the Department of Energy, Basic Energy Sciences for research support as well.

References

[1] E.A. Rohlfing, D.M. Cox, A. Kaldor, K.H. Johnson, J. Chem. Phys. 81 (1984) 3846.
[2] M.B. Knickelbein, S. Yang, J. Chem. Phys. 93 (1990) 5760.
[3] M.B. Knickelbein, S. Yang, S.J. Riley, J. Chem. Phys. 93 (1990) 94.
[4] S. Yang, M.B. Knickelbein, J. Chem. Phys. 93 (1990) 1533.
[5] M.B. Knickelbein, Chem. Phys. Lett. 192 (1992) 129.
[6] K. Athanassenas, D. Kreisle, B.A. Collings, D.M. Rayner, P.A. Hackett, Chem. Phys. Lett. 213 (1993) 105.
[7] B.A. Collings, D.M. Rayner, P.A. Hackett, Int. J. Mass Spectrom. Ion Processes 125 (1993) 207.
[8] S. Yang, M.B. Knickelbein, Z. Phys. D 31 (1994) 199.
[9] M. Knickelbein, J. Chem. Phys. 102 (1995) 1.

[10] G.M. Koretsky, M.B. Knickelbein, J. Chem. Phys. 106 (1997) 9810.
[11] L.-S. Wang, H.-S. Cheng, J. Fan, J. Chem. Phys. 102 (1995) 9480.
[12] J. Ho, K.M. Ervin, W.C. Lineberger, J. Chem. Phys. 93 (1990) 6987.
[13] H. Wu, S.R. Desai, L.-S. Wang, Phys. Rev. Lett. 76 (1996) 212.
[14] L.-S. Zheng, C.M. Karner, P.J. Brucat, S.H. Yang, C.L. Pettiette, M.J. Craycraft, R.E. Smalley, J. Chem. Phys. 85 (1986) 1681.
[15] C.L. Pettiette, S.H. Yang, M.J. Craycraft, J. Conceicao, R.T. Laaksonen, O. Cheshnovsky, R.E. Smalley, J. Chem. Phys. 88 (1988) 5377.
[16] O. Cheshnovsky, K.J. Taylor, J. Conceicao, R.E. Smalley, Phys. Rev. Lett. 64 (1990) 1785.
[17] K.J. Taylor, C.L. Pettiette-Hall, O. Cheshnovsky, R.E. Smalley, J. Chem. Phys. 96 (1992) 3319.
[18] S.K. Loh, L. Lian, P.B. Armentrout, J. Am. Chem. Soc. 111 (1989) 3167.
[19] S.K. Loh, D.A. Hales, L. Lian, P.B. Armentrout, J. Chem. Phys. 90 (1989) 5466.
[20] D.A. Hales, L. Lian, P.B. Armentrout, Int. J. Mass Spectrom. Ion Processes 102 (1990) 269.
[21] L. Lian, C.-X. Su, P.B. Armentrout, J. Chem. Phys. 97 (1992) 4084.
[22] C.-X. Su, P.B. Armentrout, J. Chem. Phys. 99 (1993) 6506.
[23] C.-X. Su, D.A. Hales, P.B. Armentrout, J. Chem. Phys. 99 (1993) 6613.
[24] D.A. Hales, C.-X. Su, L. Lian, P.B. Armentrout, J. Chem. Phys. 100 (1994) 1049.
[25] M.E. Geusic, M.D. Morse, R.E. Smalley, J. Chem. Phys. 82 (1985) 590.
[26] M.D. Morse, M.E. Geusic, J.R. Heath, R.E. Smalley, J. Chem. Phys. 83 (1985) 2293.
[27] D.J. Trevor, R.L. Whetten, D.M. Cox, A. Kaldor, J. Phys. Chem. 107 (1985) 518.
[28] R.J. St. Pierre, M.A. El-Sayed, J. Phys. Chem. 91 (1987) 763.
[29] D.M. Cox, D.J. Trevor, R.L. Whetten, A. Kaldor, J. Phys. Chem. 92 (1988) 421.
[30] Y. Hamrick, S. Taylor, G.W. Lemire, Z.-W. Fu, J.-C. Shui, M.D. Morse, J. Chem. Phys. 88 (1988) 4095.
[31] Y.M. Hamrick, M.D. Morse, J. Phys. Chem. 93 (1989) 6494.
[32] S. Nonose, Y. Sone, K. Onodera, S. Sudo, K. Kaya, J. Phys. Chem. 94 (1990) 2744.
[33] X. Ren, P. Hintz, K.M. Ervin, J. Chem. Phys. 99 (1993) 3575.
[34] S.A. Mitchell, L. Lian, P.A. Hackett, J. Chem. Phys. 103 (1995) 5539.
[35] S.A. Mitchell, D.M. Rayner, P.A. Hackett, J. Chem. Phys. 104 (1996) 4012.
[36] A. Bérces, P.A. Hackett, L. Lian, S.A. Mitchell, D.M. Rayner, J. Chem. Phys. 108 (1998) 5476.
[37] E.K. Parks, G.C. Nieman, L.G. Pobo, S.J. Riley, J. Chem. Phys. 86 (1987) 1066.
[38] B.J. Winter, T.D. Klots, E.K. Parks, S.J. Riley, Z. Phys. D 19 (1991) 381.
[39] E.K. Parks, S.J. Riley, Z. Phys. D 33 (1995) 59.
[40] E.K. Parks, G.C. Nieman, K.P. Kerns, S.J. Riley, J. Chem. Phys. 108 (1998) 3731.
[41] E.K. Parks, K.P. Kerns, S.J. Riley, J. Chem. Phys. 112 (2000) 3384.
[42] K.P. Kerns, E.K. Parks, S.J. Riley, J. Chem. Phys. 112 (2000) 3394.
[43] J. Conceição, S.K. Loh, L. Lian, P.B. Armentrout, J. Chem. Phys. 104 (1996) 3976.
[44] J.B. Griffin, P.B. Armentrout, J. Chem. Phys. 106 (1997) 4448.
[45] J.B. Griffin, P.B. Armentrout, J. Chem. Phys. 107 (1997) 5345.
[46] J.B. Griffin, P.B. Armentrout, J. Chem. Phys. 108 (1998) 8062.
[47] J.B. Griffin, P.B. Armentrout, J. Chem. Phys. 108 (1998) 8075.
[48] J. Xu, M.T. Rodgers, J.B. Griffin, P.B. Armentrout, J. Chem. Phys. 108 (1998) 9339.
[49] J.B. Hopkins, P.R.R. Langridge-Smith, M.D. Morse, R.E. Smalley, J. Chem. Phys. 78 (1983) 1627.
[50] P.R. R.Langridge-Smith, M.D. Morse, G.P. Hansen, R.E. Smalley, A.J. Merer, J. Chem. Phys. 80 (1984) 593.
[51] S. Taylor, G.W. Lemire, Y.M. Hamrick, Z. Fu, M.D. Morse, J. Chem. Phys. 89 (1988) 5517.
[52] S. Taylor, E.M. Spain, M.D. Morse, J. Chem. Phys. 92 (1990) 2710.
[53] S. Taylor, E.M. Spain, M.D. Morse, J. Chem. Phys. 92 (1990) 2698.
[54] E.M. Spain, J.M. Behm, M.D. Morse, J. Chem. Phys. 96 (1992) 2511.
[55] M. Doverstål, B. Lindgren, U. Sassenberg, C.A. Arrington, M.D. Morse, J. Chem. Phys. 97 (1992) 7087.
[56] A.M. James, P. Kowalczyk, R. Fournier, B. Simard, J. Chem. Phys. 99 (1993) 8504.
[57] A.M. James, P. Kowalczyk, B. Simard, Chem. Phys. Lett 216 (1993) 512.
[58] A.M. James, P. Kowalczyk, E. Langlois, M.D. Campbell, A. Ogawa, B. Simard, J. Chem. Phys. 101 (1994) 4485.
[59] A.M. James, P. Kowalczyk, B. Simard, J. Mol. Spectrosc. 164 (1994) 260.
[60] J.C. Pinegar, J.D. Langenberg, C.A. Arrington, E.M. Spain, M.D. Morse, J. Chem. Phys. 102 (1995) 666.
[61] C.A. Arrington, M.D. Morse, M. Doverstål, J. Chem. Phys. 102 (1995) 1895.
[62] C.A. Arrington, D.J. Brugh, M.D. Morse, M. Doverstål, J. Chem. Phys. 102 (1995) 8704.
[63] S.M. Sickafoose, J.D. Langenberg, M.D. Morse, J. Phys. Chem. A 104 (2000) 3521.
[64] E.M. Spain, M.D. Morse, J. Phys. Chem. 96 (1992) 2479.
[65] L.M. Russon, S.A. Heidecke, M.K. Birke, J. Conceicao, P.B. Armentrout, M.D. Morse, Chem. Phys. Lett. 204 (1993) 235.
[66] C.A. Arrington, T. Blume, M.D. Morse, M. Doverstål, U. Sassenberg, J. Phys. Chem. 98 (1994) 1398.
[67] L.M. Russon, S.A. Heidecke, M.K. Birke, J. Conceicao, M.D. Morse, P.B. Armentrout, J. Chem. Phys. 100 (1994) 4747.

[68] J.D. Langenberg, M.D. Morse, Chem. Phys. Lett. 239 (1995) 24.
[69] J.D. Langenberg, M.D. Morse, J. Chem. Phys. 108 (1998) 2331.
[70] M.D. Morse, G.P. Hansen, P.R.R. Langridge-Smith, L.-S. Zheng, M.E. Geusic, D.L. Michalopoulos, R.E. Smalley, J. Chem. Phys. 80 (1984) 5400.
[71] E.M. Spain, M.D. Morse, Int. J. Mass Spectrom. Ion Processes 102 (1990) 183.
[72] J.M. Behm, C.A. Arrington, M.D. Morse, J. Chem. Phys. 99 (1993) 6409.
[73] J.M. Behm, D.J. Brugh, M.D. Morse, J. Chem. Phys. 101 (1994) 6487.
[74] B. Simard, M.-A. Lebeault-Dorget, A. Marijnissen, J.J. ter Meulen, J. Chem. Phys. 108 (1998) 9668.
[75] D. Lessen, P.J. Brucat, Chem. Phys. Lett. 152 (1988) 473.
[76] R.L. Asher, D. Bellert, T. Buthelezi, G. Weersekera, P.J. Brucat, Chem. Phys. Lett. 228 (1994) 390.
[77] D. Bellert, T. Buthelezi, V. Lewis, K. Dezfulian, P.J. Brucat, Chem. Phys. Lett. 240 (1995) 495.
[78] R.L. Hettich, B.S. Freiser, J. Am. Chem. Soc. 108 (1986) 2537.
[79] J. Husband, F. Aguirre, C.J. Thompson, C.M. Laperle, R.B. Metz, J. Phys. Chem. A 104 (2000) 2020.
[80] Y.A. Ranasinghe, B.S. Freiser, Chem. Phys. Lett. 200 (1992) 135.
[81] Y. Shi, V.A. Spasov, K.M. Ervin, J. Chem. Phys. 111 (1999) 938.
[82] Z. Fu, G.W. Lemire, Y.M. Hamrick, S. Taylor, J.-C. Shui, M.D. Morse, J. Chem. Phys. 88 (1988) 3524.
[83] W.C. Wiley, I.H. McLaren, Rev. Sci. Instrum. 26 (1955) 1150.
[84] V.I. Karataev, B.A. Mamyrin, D.V. Shmikk, Sov. Phys. JETP 16 (1972) 1177.
[85] B.A. Mamyrin, V.I. Karataev, D.V. Shmikk, V.A. Zagulin, Sov. Phys. JETP 37 (1973) 45.
[86] B.A. Mamyrin, D.V. Shmikk, Sov. Phys. JETP 49 (1979) 762.
[87] U. Boesl, H.J. Neusser, R. Weinkauf, E.W. Schlag, J. Phys. Chem. 86 (1982) 4857.
[88] S. Gerstenkorn, P. Luc, Atlas du Spectre d'Absorption de la Molecule d'Iode entre 14,000–15,600 cm^{-1}, CNRS, Paris, 1978.
[89] D. Clouthier, J. Karolczak, Rev. Sci. Instrum. 61 (1990) 1607.
[90] S. Gerstenkorn, P. Luc, Atlas du Spectre d'Absorption de la Molecule d'Iode entre 14,800–20,000 cm^{-1}, CNRS, Paris, 1978.
[91] S. Gerstenkorn, P. Luc, Rev. Phys. Appl. 14 (1979) 791.
[92] P.W. Villalta, Ph.D. thesis, University of Minnesota, 1993.
[93] K.K. Baeck, R.J. Bartlett, J. Chem. Phys. 109 (1998) 1334.
[94] H. Basch, Chem. Phys. Lett. 136 (1987) 289.
[95] G. Pacchioni, P. Fantucci, J. Koutecky, Chem. Phys. Lett. 142 (1987) 85.
[96] L.G.M. Pettersson, C.W. Bauschlicher Jr., T. Halicioglu, J. Chem. Phys. 87 (1987) 2205.
[97] J.S. Tse, J. Mol. Struct. (Theochem) 165 (1988) 21.
[98] J.S. Tse, J. Chem. Phys. 92 (1990) 2488.
[99] C.W. Bauschlicher Jr., H. Partridge, S.R. Langhoff, P.R. Taylor, S.P. Walch, J. Chem. Phys. 86 (1987) 7007.
[100] K.K. Sunil, K.D. Jordan, J. Phys. Chem. 92 (1988) 2774.
[101] M.F. Cai, T.P. Dzugan, V.E. Bondybey, Chem. Phys. Lett. 155 (1989) 430.
[102] Z. Fu, G.W. Lemire, G.A. Bishea, M.D. Morse, J. Chem. Phys. 93 (1990) 8420.
[103] T.H. Upton, J. Chem. Phys. 86 (1987) 7054.
[104] A. Szabo, N.S. Ostlund, Modern Quantum Chemistry: Introduction to Advanced Electronic Structure Theory, 1st ed. revised, McGraw-Hill, New York, 1989.
[105] L. Hanley, S.A. Ruatta, S.L. Anderson, J. Chem. Phys. 87 (1987) 260.
[106] J.E. Harrington, J.C. Weisshaar, J. Chem. Phys. 93 (1990) 854.
[107] S. Anderson, University of Utah, private communication, 2000.
[108] U. Ray, M.F. Jarrold, J.E. Bower, J.S. Kraus, Chem. Phys. Lett. 159 (1989) 221.
[109] H.-P. Loock, B. Simard, S. Wallin, C. Linton, J. Chem. Phys. 109 (1998) 8980.
[110] C. Corliss, J. Sugar, J. Phys. Chem. Ref. Data 6 (1977) 1253.
[111] J.E. Sohl, Y. Zhu, R.D. Knight, J. Opt. Soc. Am. B 7 (1990) 9.
[112] E.R. Fisher, J.L. Elkind, D.E. Clemmer, R. Georgiadis, S.K. Loh, N. Aristov, L.S. Sunderlin, P.B. Armentrout, J. Chem. Phys. 93 (1990) 2676.
[113] S. Smoes, J. Drowart, High Temp. Sci. 17 (1984) 31.
[114] D.E. Clemmer, J.L. Elkind, N. Aristov, P.B. Armentrout, J. Chem. Phys. 95 (1991) 3387.
[115] J. Sugar, C. Corliss, J. Phys. Chem. Ref. Data 7 (1978) 1191.
[116] D.S. Yang, A.M. James, D.M. Rayner, P.A. Hackett, J. Chem. Phys. 102 (1995) 3129.
[117] S.P. Walch, C.W. Bauschlicher Jr., J. Chem. Phys. 83 (1985) 5735.
[118] S.P. Walch, C.W. Bauschlicher Jr., in Quantum Chemistry: The Challenge of Transition Metals and Coordination Chemistry, A. Veillard (Ed.), Reidel, Dordrecht, 1986, p. 119.
[119] D.S. Yang, A.M. James, D.M. Rayner, P.A. Hackett, Chem. Phys. Lett. 231 (1994) 177.
[120] R.L. Asher, D. Bellert, T. Buthelezi, P.J. Brucat, Chem. Phys. Lett. 224 (1994) 529.
[121] L. Lian, C.-X. Su, P.B. Armentrout, Chem. Phys. Lett. 180 (1991) 168.
[122] C.E. Moore, Atomic Energy Levels, Natl. Bur. Stand. U.S. Circ. No. 467, U.S. GPO, Washington, DC, 1971.
[123] M. Doverstål, L. Karlsson, B. Lindgren, U. Sassenberg, J. Phys. B 31 (1998) 795.
[124] R.J. Van Zee, W. Weltner, Jr., Chem. Phys. Lett. 107 (1984) 173.
[125] R.J. Van Zee, S. Li, W. Weltner Jr., J. Chem. Phys. 103 (1995) 2762.
[126] A. Kant, S.-S. Lin, J. Chem. Phys. 51 (1969) 1644.
[127] Y.M. Efremov, A.N. Samoilova, V.B. Kozhukhovsky, L.V. Gurvich, J. Mol. Spectrosc. 73 (1978) 430.
[128] S.K. Gupta, R.M. Atkins, K.A. Gingerich, Inorg. Chem. 17 (1978) 3211.
[129] R.J. Van Zee, W. Weltner, Jr., High Temp. Sci. 17 (1984) 181.

[130] R.J. Van Zee, W. Weltner Jr., Chem. Phys. Lett. 150 (1988) 329.
[131] S.M. Sickafoose, D.A. Hales, M.D. Morse, Can. J. Phys., in press.
[132] M. Cheeseman, R.J. Van Zee, W. Weltner Jr., High Temp. Sci. 25 (1988) 143.
[133] D.A. Hales, P.B. Armentrout, J. Cluster Sci. 1 (1990) 127.
[134] K. Balasubramanian, D.-W. Liao, J. Phys. Chem. 93 (1989) 3989.
[135] K.A. Gingerich, D.L. Cocke, J. Chem. Soc. Chem. Commun. (1972) 536.
[136] D.L. Cocke, K.A. Gingerich, J. Chem. Phys. 60 (1974) 1958.
[137] H. Wang, H. Haouari, R. Craig, Y. Liu, J.R. Lombardi, D.M. Lindsay, J. Chem. Phys. 106 (1997) 2101.
[138] I. Shim, K.A. Gingerich, in Physics and Chemistry of Small Clusters, P. Jena, B.K. Rao, S.N. Khanna (Ed.), Series B: Physics Vol. 158, Plenum, New York and London, 1987.
[139] E.M. Spain, M.D. Morse, J. Chem. Phys. 97 (1992) 4641.
[140] A. Kant, J. Chem. Phys. 41 (1964) 1872.
[141] K. Balasubramanian, J. Chem. Phys. 87 (1987) 6573.
[142] S.K. Gupta, B.M. Nappi, K.A. Gingerich, Inorg. Chem. 20 (1981) 966.